FEATURE ARTICLE

Probing Free Multiply Charged Anions Using Photodetachment Photoelectron Spectroscopy

Lai-Sheng Wang* and Xue-Bin Wang

Department of Physics, Washington State University, 2710 University Drive, Richland, Washington 99352, and W. R. Wiley Environmental Molecular Sciences Laboratory, MS K8-88, P.O. Box 999, Pacific Northwest National Laboratory, Richland, Washington 99352

Received: November 12, 1999; In Final Form: December 23, 1999

Multiply charged anions are common in the condensed phase, and their existence has been generally taken for granted. But until very recently, these species have only rarely been observed in the gas phase. A new experimental technique, using photodetachment photoelectron spectroscopy, electrospray, and ion-trap mass spectrometry, has been developed in the author's laboratory to probe multiply charged anions in the gas phase. In this article, the principles of this technique and some of the initial results will be presented and discussed. The difference between photodetachment of singly and multiply charged anions is emphasized. Photodetachment photoelectron spectroscopy is ideal to probe the chemical and physical properties of free multiply charged anions. Among the initial findings, the repulsive Coulomb barriers existing in multiply charged anions have been directly observed. The relationship between the intramolecular electron−electron repulsion and the potential barrier is elucidated, culminating in the first observation of a negative electron binding energy in a quadruply charged anion. Electron tunneling effects through the repulsive Coulomb barriers are also observed and interpreted using a model Coulomb potential and the theory developed to understand α-decay in nuclear physics. We show that the electrospray technique provides a unique means that allow solution phase species and chemistry to be investigated in the gas phase with molecular details and specificity but without the complication of the condensed phase environments.

1. Introduction

Photoionization of a neutral molecule produces a positive ion and an outgoing electron (Figure 1a); photodetachment of a singly charged molecular anion also produces an outgoing electron and a neutral molecule (Figure 1b). In both cases, the long-range interactions between the photoproducts are attractive in nature. However, photodetachment of a multiply charged anion (MCA) results in two negatively charged particles (a free electron and a negative ion with one less charge than the parent MCA), whose long-range interactions are mainly the Coulomb repulsion (Figure 1c). The superposition of the short-range binding of the electron and the long-range Coulomb repulsion gives rise to a potential barrier for the outgoing electron, as schematically shown in Figure 2a for a hypothetical MCA (AB^{n-}). This repulsive Coulomb barrier (RCB) was inferred in studies of multiply charged clusters and fullerene anions.[1−7] The RCB in MCA's is analogous to the potential barrier binding the α-particles in a radioactive atomic nucleus,[8] even though the length and energy scales are quite different in the two cases.

The RCB has profound effects on the properties of MCA's and is expected to lead to interesting phenomena in photodetachment experiments. For example, Wigner's threshold law[9] of photodetachment would not hold and threshold photodetachment of MCA's is simply not feasible any more. Thus one has the interesting situation, where, if the detachment photon energy is below the RCB, no electron detachment will occur even if the photon energy is above the asymptotic electron binding energy (see Figure 2a). In this case, detachment can only take place through electron tunneling, which at threshold would have negligible probability. Therefore, determination of the excess electron binding energies (BE, Figure 2a) of MCA's can only

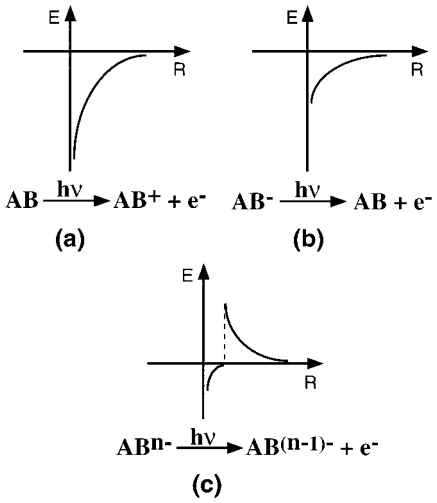

Figure 1. Schematic potential energy curves for (a) photoionization of a neutral molecule, (b) photodetachment of a singly charged anion, and (c) photodetachment of a multiply charged anion. Note the long-range Coulomb repulsion in (c).

10.1021/jp9940093 CCC: $19.00
Published on Web 02/18/2000

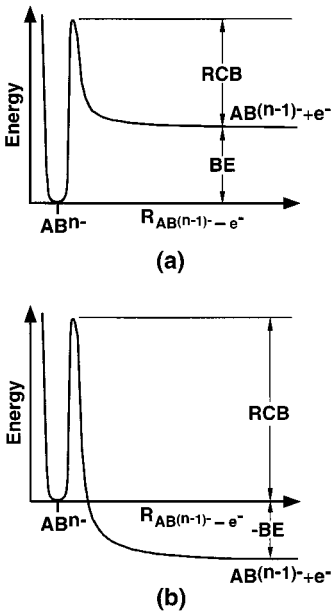

Figure 2. Schematic potential energy curves showing the excess electron binding energy (BE) and the repulsive Coulomb barrier (RCB) in multiply charged anions: (a) for an electronically stable multiply charged anion with a positive BE; (b) for an electronically unstable multiply charged anion with a negative BE.

be accomplished through photoelectron spectroscopy (PES) using photon energies higher than the RCB, since Einstein's photoelectric equation still holds: $h\nu = \mathrm{KE} + \mathrm{BE}$, where $h\nu$ is the photon energy, KE is the outgoing electron kinetic energy, and BE is the electron binding energy. Photoelectron kinetic energies (KE) are measured in PES; the electron binding energies (BE) are thus determined straightforwardly. Such PES experiments have recently been performed for the first time in our laboratory for a number of MCA's.[10−21] By performing photon-energy-dependent PES experiments, we have observed directly the effects of the RCB and electron tunneling. We have also determined the magnitude of the RCB and elucidated the electrostatic interactions and electronic stability of MCA's and their relationship to the RCB.

Even more interesting is the situation when the long-range Coulomb repulsion is stronger than the short-range electron binding, resulting in metastable MCA's (Figure 2b). Such species may exist because of the RCB, which can render substantial lifetimes to the metastable MCA's. Basically, in this case, the $AB^{(n-1)-}$ anion is electronically more stable than the AB^{n-} MCA, which thus possesses a negative electron binding energy (Figure 2b). This would result in an unusual phenomenon in PES experiments that the outgoing electron kinetic energy would be higher than the incoming photon energy (Einstein's photoelectric equation is still valid!). The extra energy derives from the electrostatic energy stored in the AB^{n-} MCA. Such metastable MCA's with negative electron binding energies have been recently observed in our laboratory, and the magnitudes of the negative binding energies are directly measured from PES experiments.[18−20]

Multiply charged anions are ubiquitous in nature and are important constituents in solutions and solids. Their existence has been generally taken for granted in the teaching of chemistry and our understanding of materials. However, free MCA's have been difficult to study and very few of them have been known in the gas phase previously.[1,2,22−25] This is partly due to the fact that many MCA's acquire their stability in the condensed phase through solvation and other electrostatic interactions and are not stable in the gas phase. Experimentally, the few MCA's observed in the gas phase were all through mass spectrometry. Doubly charged anions were first observed with large organic molecules,[26−30] where the two excess charges are well separated, reducing the Coulomb repulsion. The observation of small carbon cluster dianions, C_n^{2-} ($n = 7-28$), by Compton et al. using a sputtering source,[32] has stimulated much recent experimental and theoretical interests in gaseous MCA's. Doubly charged anions have since been observed in a number of systems, including small carbon clusters,[33−36] fullerenes,[37−39] and other species,[40−42] primarily using the ion sputtering technique. Kerbarle and co-workers,[43−45] as well as others,[46−51] have used electrospray to produce a number of doubly charged small organic, inorganic, and fullerene anions, which exist in liquid solutions.

Theoretical investigations of MCA's have also been very active recently.[2] Early theoretical considerations of MCA's derived from interests in searching for molecular species with unusually high electron affinities (EA's)[52−57] and in understanding electronic structure of condensed phase species.[58−60] Interestingly, Gutsev and Boldyrev even proposed formulas to search for the highest possible second and higher order EA's.[54] Major theoretical advances in MCA's have been made lately by the groups of Cederbaum and Simons. Cederbaum and co-workers[61−76] have investigated a series of gaseous MCA's and proposed a "construction principle" for predicting gaseous MCA's on the basis of the alkali-metal and alkaline-earth-metal halide systems.[65−67] They have predicted a number of other interesting cluster dianions, some of which have been recently observed in mass spectrometric studies.[41,42] Simons and co-workers have considered many MCA's that exist in the condensed phase and investigated their structure, bonding, and stability in the gas phase.[77−83] There have also been a number of other theoretical studies on gaseous MCA's,[84−96] in particular concerning small carbon clusters[86−90] and those relevant to condensed phase materials.[91−96] The electron−electron repulsion and the resultant RCB have been considered in several theoretical works on multiply charged metal cluster and fullerene anions.[5−7,97−99]

Photoelectron spectroscopy is a powerful experimental technique to probe the electronic structure of matter.[100−102] It has been widely used to study singly charged anions,[103−110] providing information about electron affinities and low-lying electronic states for a vast number of neutral species and clusters. We have recently developed a PES apparatus designed to investigate multiply charged anions in the gas phase, using electrospray and ion-trap mass spectrometry.[16] PES is an ideal technique to investigate the intrinsic properties of multiply charged anions in the gas phase. It provides direct measurements of the excess electron binding energies in multiply charged anions, thus allowing information about their stability and intramolecular Coulomb repulsion to be obtained. Photon-energy-dependent studies also allow the RCB and electron tunneling to be investigated. Many inorganic metal-complex anions can now be studied in the gas phase using PES, which will provide detailed molecular electronic structure information about these solution species. More importantly, the electrospray technique provides a general tool, which allows solution phase species and processes to be investigated in the gas phase. In this article, some of our initial results[10−21] in this new endeavor will be discussed.

2. Experimental Methods

The difficulty in studying MCA's lies at their formation in the gas phase. Even if a doubly charged anion is stable as a

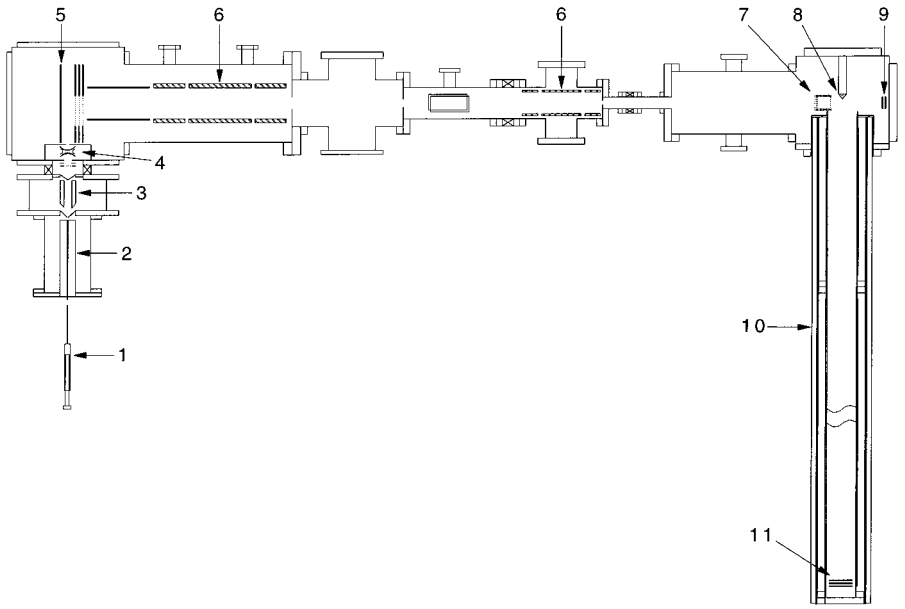

Figure 3. Schematic view of the electrospray-photodetachment apparatus. Key: 1, syringe; 2, heated desolvation capillary; 3, radio frequency quadrupole ion guide; 4, quadrupole ion-trap; 5, time-of-flight mass spectrometer extraction stack; 6, Einzel lens assembly; 7, three-grid mass-gate and momentum decelerator assembly; 8, permanent magnet (NdFeB); 9, 40-mm dual microchannel plates in-line ion detector; 10, 4-m time-of-flight tube with a low field solenoid and double layer μ-metal shielding; 11, 18-mm Z-stack microchannel plates photoelectron detector. From ref 16.

gaseous species, it would still be fairly challenging to make it through sequential electron attachments in the gas phase, because of the long-range Coulomb repulsion between the initially singly charged anion and the second electron. Although a number of doubly charged anions have been observed using ion sputtering and other collisional techniques,[32−42] there is not a general experimental technique to produce gaseous multiply charged anions. However, recently the electrospray ionization technique, pioneered by Fenn and co-workers,[111−113] has been shown not only to be a powerful soft-ionization method for biomolecules[114] but also to be able to produce small gaseous MCA's from solutions.[43−47] In electrospray, one starts with a solution sample containing the MCA's of interests. The solution is sprayed through a syringe needle biased at a negative high voltage, producing highly charged liquid droplets at ambient conditions. The liquid droplets are broken down in a heated bath gas or capillary, in which the solvent molecules are removed (desolvation) and the intended MCA's are thus formed out of the liquid droplets. The limitation of the electrospray technique is that the MCA of interest has to be present in the original solution. The advantage is that one avoids the sequential electron attachment processes and it is generally applicable to a wide range of MCA's so long as they exist in a solution and are long-lived in the gas phase.

The apparatus that we have developed couples an electrospray ion source with a magnetic-bottle time-of-flight (TOF) photoelectron analyzer.[106,110] Details of this apparatus have been published,[16] and Figure 3 gives a schematic overview. Typically, a water/methanol (2/98 ratio) mixed solution containing the anions of interest is sprayed at ambient conditions through a fine syringe (1), which is biased at a negative high voltage. The highly charged liquid droplets produced are fed into a desolvation capillary (2) heated to 50−100 °C. The molecular anions emerged from the desolvation capillary are guided by a RF-only quadupole system (3) into a quadrupole ion-trap (4). The anions are usually accumulated for about 0.1 s before being pushed out into a TOF mass spectrometer (5, 6, 9) for mass and charge analyses. The desired anions are selected by a mass gate and decelerated (7) before being detached by a laser beam in the interaction zone of the magnetic-bottle PES analyzer (8, 10, 11). A number of detachment photon energies are used, ranging from a Nd:YAG laser (532, 355, 266 nm) to an excimer laser (193 and 157 nm). The photoemitted electrons are collected at nearly 100% efficiency by the magnetic bottle and analyzed by the 4-m-long electron flight tube (10). The ion-trap and TOF mass spectrometer are operated at 10 Hz repetition rate while the magnetic-bottle PES analyzer is operated at 20 Hz with the ion beam off at alternating laser shots for background subtraction, which is necessary at 266, 193, and 157 nm detachment wavelengths. The photoelectron kinetic energies are usually calibrated with the known spectra of O^- and I^-. The resolution of the magnetic-bottle PES analyzer is about 2% (ΔKE/KE), i.e., ~10 meV for 0.5 eV electrons.

3. Highlights of Recent Work

3.1. Direct Observation of the Repulsive Coulomb Barrier. The first PES experiment was performed on the citrate dianion (CA^{2-}; see Figure 4a for structure).[10] Figure 5a shows the spectrum of CA^{2-} at 355 nm (3.496 eV), where one broad band (X) was observed with an estimated adiabatic electron binding energy of 1.0 eV. Figure 5b displays the spectrum of CA^{2-} at 266 nm (4.661 eV), where an even broader spectrum was observed. Close examination of the 266-nm spectrum revealed that it actually contained two overlapping bands, the X-band observed in the 355-nm spectrum and another band at a higher binding energy (A), as seen more clearly in Figure 5c. The A-band was estimated to be ~0.6 eV higher in binding energy than the X-band. We also attempted to take the PES spectrum of CA^{2-} at 532 nm (2.331 eV). However, no photoelectron signals were observed even though the 2.331-eV photon energy was higher than the binding energies of both the X and A bands.

The photodetachment transitions take place between the ground state of CA^{2-} and the ground and excited states of the CA^- singly charged anion. The X-band represents the ground state of CA^-; the discernible fine features in Figure 5a are due to partially resolved vibrational structures. The spectral width (the Franck−Condon envelope) is a measure of the geometry

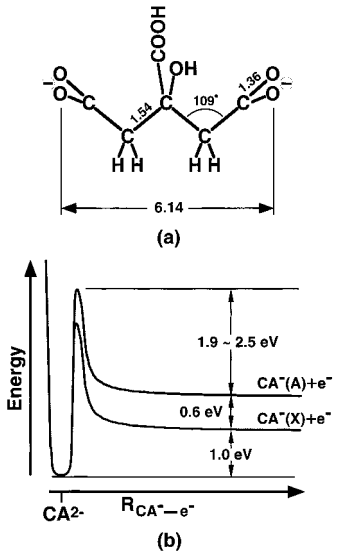

Figure 4. (a) Schematic structure of the citrate dianion with relevant bond lengths (Å) and bond angles (deg). (b) Schematic potential energy curves showing the adiabatic binding energies and the repulsive Coulomb barrier for detachment of CA^{2-}, leading to the X and A asymptotic states of CA^{-}. Note that the barrier heights relative to the X and A states are assumed to be the same. From ref 10.

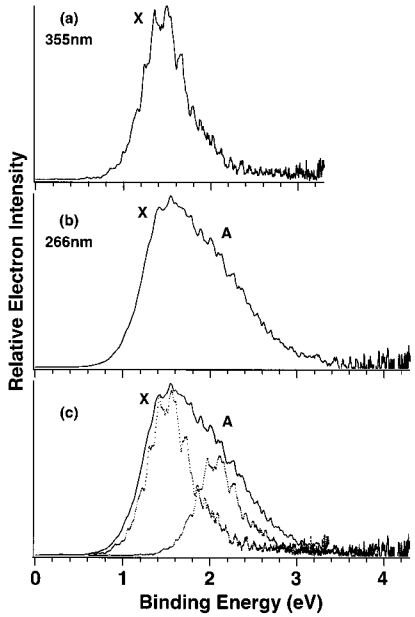

Figure 5. Photoelectron spectra of citrate dianion (CA^{2-}) at (a) 355 nm (3.496 eV) and (b) 266 nm (4.661 eV). Note the increased spectral width in the 266-nm spectrum, implying an additional detachment channel as shown in (c). From ref 10.

changes between the dianion and the singly charged anion. The A-band then is due to the first excited state of CA^{-}.

Figure 5 vividly demonstrates the effects and the first direct observation of the RCB. The photon-energy-dependent spectra can be understood with the help of the schematic potential curves in Figure 4b, where the binding energies of the two observed states (X and A) are shown. There exists a RCB for each state. The 266-nm photon must be above the RCB of both the X and A states, so both these states are observable at 266 nm. The 355-nm photon must be below the RCB of the A-state but higher than that of the X-state, so only the X-state is accessible at 355 nm. The 532-nm photon must then be lower than the RCB of both the X and A states; thus, no signal can be observed at this photon energy. If the RCB's of the X and A states are assumed to be the same, they can be estimated (bracketed) based on the above photon-energy-dependent information. The RCB of CA^{2-} is estimated to be $1.9 < \text{RCB} < 2.5$ eV, as given in Figure 4b.

The two charges are known to be localized on the two terminal carboxyl groups in CA^{2-} (Figure 4a). The distance between the two charge centers, assumed to be the terminal O−O distance, is estimated to be ~6.14 Å, as shown in Figure 4a. We thus estimate a Coulomb repulsion energy ($e^2/4\pi\epsilon_0 r$) of about 2.3 eV, which is right in the range of the RCB determined experimentally. This observation suggested that the magnitude of the RCB is related to the intramolecular Coulomb repulsion energy.

3.2. Intramolecular Electron−Electron Repulsion and the Repulsive Coulomb Barrier. The citrate dianion is an ideal system to understand the intramolecular Coulomb repulsion because the two negative charges are localized and their spatial relationship is known. Its two detachment bands (Figure 5) are due to removal of electrons from one of the carboxylate groups. The above discussion suggests that the intramolecular Coulomb repulsion estimated from the known molecular structural parameters is approximately equal to the magnitude of the RCB in the CA^{2-} dianion. This is a significant observation because if this is true the relationship between the RCB and the intramolecular Coulomb repulsion can be understood. In particular, one can then quantitatively determine the magnitude of the intramolecular Coulomb repulsion in MCA's through measurements of the magnitudes of the RCB. This would be especially valuable for MCA's whose charge distributions are more complicated or even delocalized.

To confirm the above observation, we performed PES experiments on a series of linear dicarboxylate dianions (DC^{2-}), $^{-}O_2C-(CH_2)_n-CO_2^{-}$, where n indicates the aliphatic chain length.[11] These dianions are similar to the citrate dianion, and the two charges are localized on the terminal carboxyl groups, but now the separation between the two charges can be systematically varied. We expected that the electron binding energies of these dianions would increase with n and extrapolate to that of a singly charged $X-CO_2^{-}$ species (X represents an aliphatic group), when n approaches infinity. Similarly, the RCB should decrease with n and extrapolate to zero as n approaches infinity.

Figure 6 shows the PES spectra of a series of DC^{2-}, with $n = 3-10$, at two photon energies, 266 and 355 nm.[11] Several observations can be made immediately. First, two spectral features (X and A) are observed in the 266-nm spectra, similar to that of CA^{2-} (Figure 5), except that the two features are better separated for the DC^{2-} dianions. Second, indeed the electron binding energies increase with n. Third, the A-band disappears in the 355-nm spectra due to the RCB, which can be similarly understood using the potential energy curves of Figure 4b. Again, if we assume that the RCB has the same magnitude for the X and A states, we can estimate the RCB for each DC^{2-} anion using a similar bracketing procedure, as done for the CA^{2-} dianion.

Figure 7 shows the adiabatic electron binding energies (EBx) and the estimated RCB's as a function of $1/r_n$, where r_n is the distance between the terminal O−O in DC^{2-} (also see Figure 4a) and obtained through ab initio calculations.[11] The top axis shows the chain length index, n. Interestingly, we observed that both the binding energies and the RCB's are dependent on $1/r_n$ linearly. A least-squares fit of the EBx curve gives the following: $\text{EBx} = 3.21 - 16.7/r_n$. The 3.21 eV value, when r_n approaches infinity, is consistent with our measured binding energy of 3.4 eV for a singly charged carboxylate anion

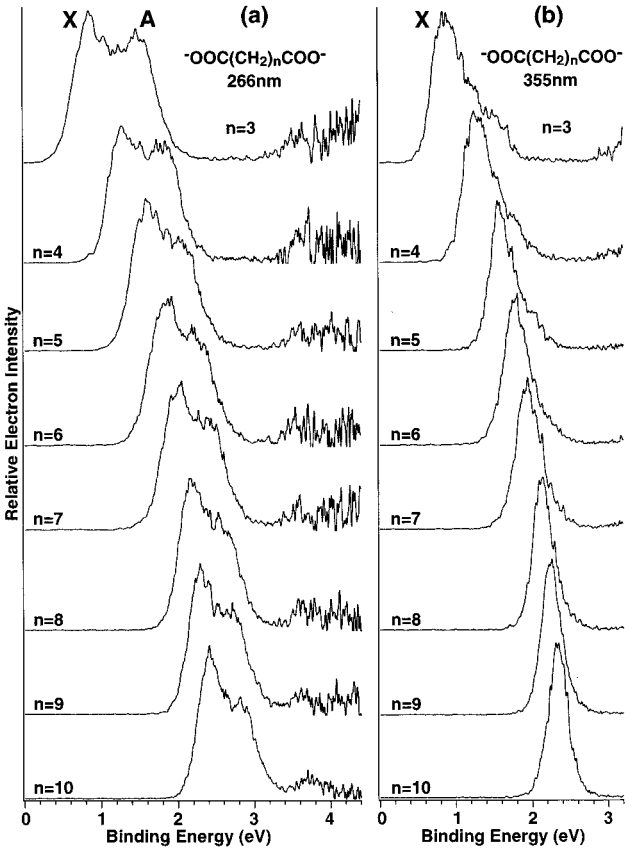

Figure 6. Photoelectron spectra of $^{-}O_2C-(CH_2)_n-CO_2^{-}$ (DC^{2-}) dianions ($n = 3-10$) at (a) 266 nm (4.661 eV) and (b) 355 nm (3.496 eV). From ref 11.

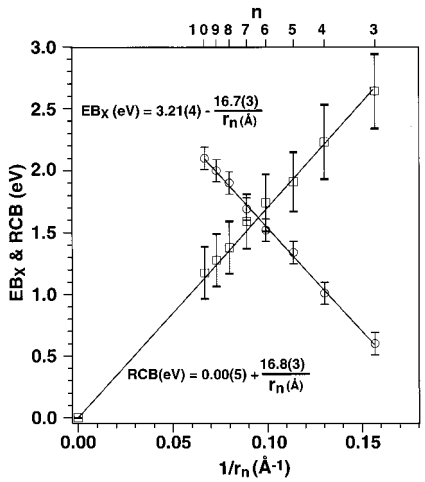

Figure 7. Measured adiabatic electron binding energies (EB_x) and the estimated repulsive Coulomb barrier (RCB) heights for $^{-}O_2C-(CH_2)_n-CO_2^{-}$ (DC^{2-}) dianions ($n = 3-10$) as a function of $1/r_n$, where r_n is the average equilibrium distance (Å) between the two charge centers in DC^{2-}, assumed to be localized on the O atoms of the carboxylate groups. Key: circles, EB_x; squares, RCB; lines, least-squares fits. From ref 11.

$CH_3CO_2^{-}$.[11] The RCB curve indeed goes through the origin. That is, at infinitive charge separation, there is no intramolecular Coulomb repulsion, and consequently, there would be no RCB.

We note that the coefficients of the EBx and RCB curves have the same magnitude with opposite signs. This leads to the interesting result, EBx + RCB = 3.21 eV. Referring to Figure 2a and Figure 4b, we note that EBx + RCB is the potential well that effectively binds the electron relative to the ground state (X) of the singly charged anion. This result means that the potential wells for all the DC^{2-} dianions are the same and this potential well is equivalent to the binding energy of an electron to a carboxyl group. Therefore, the decrease of the binding energy in the dianions, due to the presence of the second charge (intramolecular Coulomb repulsion), is equal exactly to the RCB. This result unequivocally confirmed that the magnitude of the RCB in MCA's is equal exactly to the amount of intramolecular Coulomb repulsion. This conclusion should be generally applicable to all MCA's.

The value of the coefficient (16.7 eV Å) in the curves of Figure 7 is somewhat unusual. With a dielectric constant of one (for vacuum), the coefficient for the Coulomb repulsion ($e^2/4\pi\epsilon_0 r$) should be 14.4 eV Å. The 16.7 eV Å value would indicate a dielectric constant less than one. Yet the dielectric constant of bulk saturated hydrocarbon is ~2.[115] Previous studies of proton affinities in $^{+}H_3N-(CH_2)_n-NH_3^{+}$ dications, which have a similar intramolecular Coulomb repulsion between the two protons, have concluded that the effective dielectric constant in these systems is approximately one.[116] Our current observation is consistent with this previous result. Our obtained coefficient of 16.7 eV Å, which is larger than the expected value of 14.4 eV Å, is caused by the charge delocalization over the carboxyl groups in the DC^{2-} dianions, resulting in a uncertainty in determining the charge separations.[11] The O−O distances used in the plot of Figure 7 overestimated the true distances between the two charges. If slightly smaller O−O distances were to be used, the 14.4 eV Å coefficient could be recovered. A recent theoretical study, concerning the effective dielectric constants using different spacer groups in doubly charged ions, confirmed our current observation and interpretation.[117]

3.3. Electron Tunneling through the Repulsive Coulomb Barrier. Analogous to the α-decay phenomenon,[8] quantum tunneling effects are expected to occur through the RCB when the detachment photon energies are above the asymptotic binding energy of an MCA but below the RCB. Indeed, such tunneling effects have been observed in the DC^{2-} anions at 532 nm and have been studied quantitatively using the WKB formalism developed for α-decay theory.[15,19]

Figure 8 shows the PES spectra of DC^{2-} (for $n = 3-5$) at 532 nm, compared to that at 355 nm. The schematic potential energy curves in each case are also shown with the necessary energetic information. It is seen that the 532-nm photon is below the RCB in all cases (top of Figure 8); thus, any signals observed at this photon energy have to be due to electron tunneling or a two-photon process. The latter was eliminated through photon-flux dependent studies. The signals at 532 nm are indeed much weaker, consistent with the tunneling mechanism. Interestingly, the signals also decrease as n increases, with negligible tunneling signals observed for the dicarboxylate dianions ($^{-}O_2C-(CH_2)_n-CO_2^{-}$) with $n > 5$. Another puzzling observation was that the 532-nm spectra seem to shift to lower binding energies relative to the 355-nm spectra and the shift increases as n increases, as indicated by the vertical lines in Figure 8. From the potential curves shown in Figure 8, we see that the position of the 532-nm photon has the same distance to the RCB top in all cases, because the well depth is the same for all the DC^{2-} dianions. The only difference is that the electron kinetic energies corresponding to the detachment features in each case decrease with n, because the binding energies increase with n.

The potential energy between the outgoing electron and the singly charged anion, DC^{-}, is determined by their Coulomb repulsion at long range and the electron binding energy to DC^{-} at short range. The exact shape of the short-range potential is

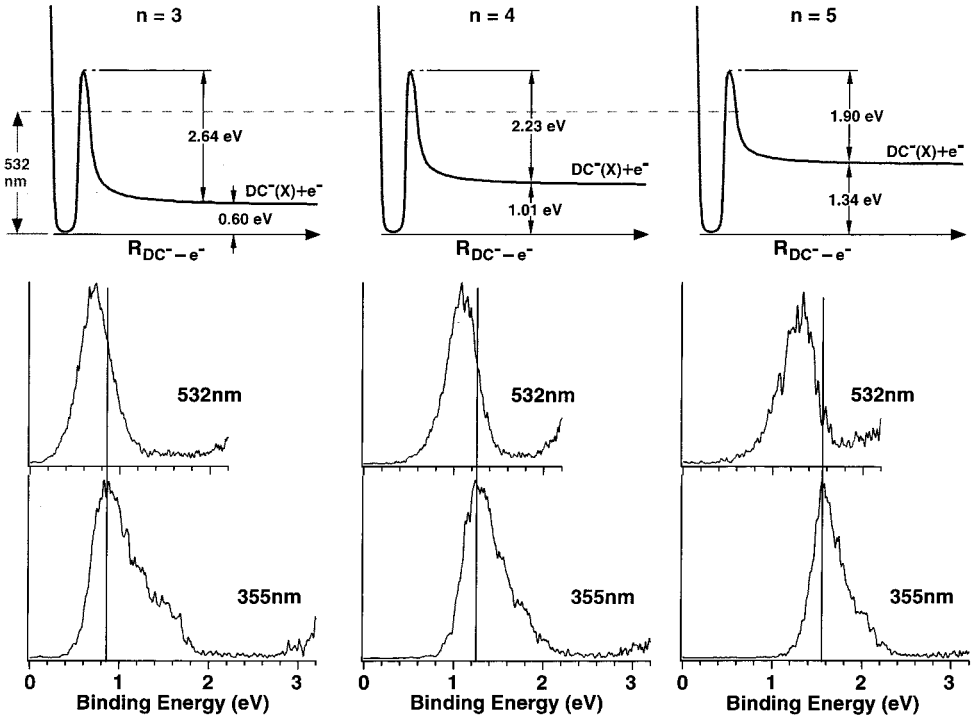

Figure 8. Comparison of the 532-nm (2.331 eV) photoelectron spectra of DC^{2-} ($n = 3-5$) to those taken at 355 nm. Top: schematic potential energy curves corresponding to the ground state of the DC^- singly charged anions, with the respective adiabatic binding energies and barrier heights. The position of the 532-nm photon is shown in the potential energy curves. The shift of the 532-nm spectra relative to the 355-nm spectra, as indicated by the vertical lines, is due to the electron tunneling effects.

not known and would require a rigorous quantum treatment. To understand the observed electron tunneling phenomenon, we choose to use a very simple model potential, as shown in Figure 9. This potential is entirely analogous to the nuclear potential used in the α-decay theory.[8] Here the short-range potential is modeled as a square well: V_0 is the binding energy of the outgoing electron, which is measured experimentally, and R is the equilibrium distance between the two charges in DC^{2-}, taken as the terminal O−O distances. The value of α should be 14.4 ($e^2/4\pi\epsilon_0 R$), if we use the unit of eV for energy and Å for distance. However, we take the α value as 16.8, as derived above,[11] since we use the terminal O−O distance as the charge separation. The larger α value is due to the fact that the two charges are not point charges but rather slightly delocalized, as discussed above. This potential should be a good approximation since the tunneling effects we are interested occur well below the barrier top. According to the WKB approximation,[8] the tunneling probability can be calculated as:

$$T = \exp\left[-\frac{2}{\hbar}\left|\int_R^{R'} \sqrt{2m(E - V(r))}\, dr\right|\right] \quad (1)$$

where R and R' define the width of the RCB at energy E, as shown in Figure 9, m is the mass of the electron, and $\hbar$ is the Planck constant. Using our model potential, eq 1 is reduced to[8]

$$T = \exp\left[-\frac{2}{\hbar}\alpha\sqrt{\frac{2m}{\hbar}}\left(a\cos\sqrt{\frac{ER}{\alpha}} - \sqrt{\frac{ER}{\alpha}\left(1 - \frac{ER}{\alpha}\right)}\right)\right] \quad (2)$$

The kinetic energy of the outgoing electron, E, is equal to the detachment photon energy (532 nm, 2.33 eV) minus the electron binding energy in each case.

Since the tunneling probability depends on the electron kinetic energy exponentially, it is easy to understand the decrease of tunneling signals as n increases. For the transition to the ground vibrational level, we calculated a transmission probability of

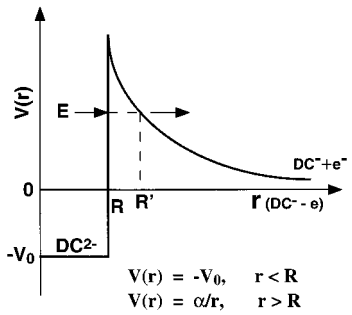

Figure 9. Coulomb potential used to calculate electron tunneling in photodetachment of DC^{2-} at 532 nm. Here the short-range potential is modeled as a square well. V_0 is the binding energy of the outgoing electron, as measured from the PES spectra. R is the equilibrium distance between the two charges in DC^{2-}. α is a constant taken as 16.8 eV Å (see Figure 7).[11] E is the kinetic energy of the outgoing photoelectron. From ref 15.

12%, 8%, 4%, and 0% for $n = 3$, 4, 5, and 6, respectively. The tunneling probabilities decrease rapidly for the larger DC^{2-} dianions, in excellent agreement with the experimental observation (Figure 8).

We also note that the 532-nm spectra all seem to shift to lower binding energies. This is due to the decreased tunneling probabilities for the higher vibrational features (which correspond to lower electron kinetic energies) and the presence of hot band transitions (which correspond to higher electron kinetic energies). In other words, in the tunneling regime, the observed spectra do not represent the normal Franck−Condon envelope, because the Franck−Condon factors of the different vibrational levels are modified by the tunneling probabilities. The hot band transitions, resulting in slightly higher photoelectron kinetic energies, tend to have higher tunneling probabilities, giving the appearance of the spectral shift at 532 nm relative to the spectra at 355 nm, where tunneling does not play a role. This situation is more easily understandable if we normalize the intensities of

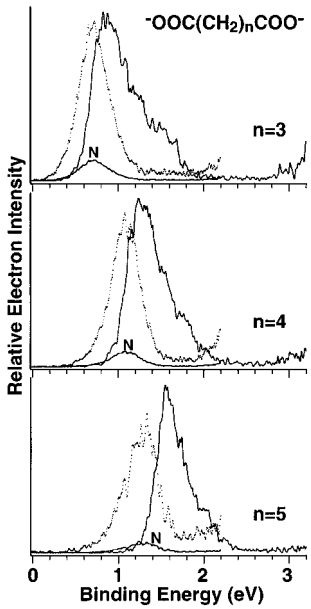

Figure 10. Comparison of the unnormalized (dotted) and normalized (N) 532-nm spectra to the 355-nm spectra, showing that the spectral shift at 532 nm was really due to the fact that different vibrational levels, corresponding to slightly different electron kinetic energies, have different tunneling probabilities. From ref 15.

the 532-nm spectra relative to the 355-nm spectra, as shown in Figure 10. This result suggests that at finite temperatures PES features resulting from tunneling cannot yield true measures of the electron binding energies. Sufficiently high photon energies are necessary to make sure that there is no tunneling bias on the PES features. Another significant finding of the tunneling calculations is that if the photon energy is only slightly above the asymptotic electron binding energy, the tunneling probability was shown indeed to be negligible as are the cases for $n > 6$ at 532 nm, thus making threshold photodetachment impossible for MCA's.

3.4. Observation of Negative Electron Binding Energy. According to Figure 2b, it is possible to have MCA's with negative electron binding energies. In fact, this is the case for many familiar textbook MCA's, such as SO_4^{2-}, CO_3^{2-}, and PO_4^{3-}, which have so high negative electron binding energies as to rendering them unstable in the gas phase.[79] Boldyrev and Simons have calculated that SO_4^- is more stable than SO_4^{2-} by more than 1.34 eV and declared that "Isolated SO_4^{2-} and PO_4^{3-} Anions Do No Exist".[79] Indeed these MCA's have never been observed in the gas phase because of the small sizes of the anions and the facile electron autodetachment. To discover MCA's with negative binding energies and substantial lifetimes, one needs to look in larger molecular systems. One obvious target is C_{60}^{2-}, which has been observed to be long-lived in the gas phase[37,38] and predicted theoretically to have a negative binding energy as much as 0.3 eV.[2,5,7,98,99] However, we were not successful in producing C_{60}^{2-} with our electrospray source. Other groups also failed to observe C_{60}^{2-} using electrospray;[118] the previous sightings of C_{60}^{2-} were both done with laser desorption in an ion-cyclotron resonance mass spectrometer.[37,38]

Our first successful observation of a negative binding energy[18] came as a complete surprise in a quadruply charged anion, copper phthalocyanine, 3,4′,4″, 4‴-tetrasulfonate $[CuPc(SO_3)_4]^{4-}$, as shown in Figure 11.[119] This MCA was produced abundantly by electrospray of a sodium salt solution. Both monosodiumated and monoprotonated triply charged anions were also observed.[20] Figure 12a,b shows the spectra of $[CuPc(SO_3)_4]^{4-}$ tetraanions

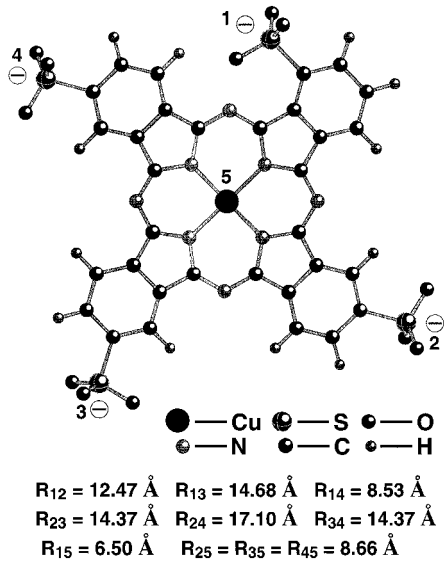

Figure 11. Structure of the $[CuPc(SO_3)_4]^{4-}$ tetraanion as determined in bulk crystals.[119] The location of the charges and the distances between the charge centers and between the charge centers and the central Cu atom are shown. Structural optimization using the semiempirical method gives similar structural parameters.[20]

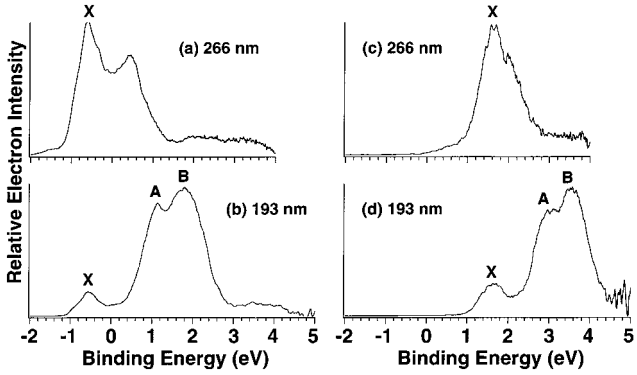

Figure 12. Photodetachment spectra of $[CuPc(SO_3)_4]^{4-}$ and $[CuPc(SO_3)_4H]^{3-}$ at 266 and 193 nm: (a, b) $[CuPc(SO_3)_4]^{4-}$; (c, d) $[CuPc(SO_3)_4H]^{3-}$. Note the negative electron binding energy feature (X) of the tetraanion and the rigid shift to higher binding energies of the trianion spectra. From ref 18.

at 266 and 193 nm.[18] The 193-nm spectrum reveals a weak feature (X) at negative binding energies with a threshold energy of −0.9 eV and two broad features (A and B) at higher binding energies. The observation of the negative binding energy feature is remarkable, indicating the photoelectron kinetic energy corresponding to this feature is 7.32 eV at 193 nm, i.e., 0.9 eV higher than the photon energy! At 266 nm, the negative binding energy feature becomes dominant; the higher binding energy feature B disappears, and only a tail of the feature A is observed. Figure 12c,d shows the spectra of the triply charged monoprotonated species, $[CuPc(SO_3)_4H]^{3-}$, at 266 and 193 nm. The features of the 193-nm spectrum of the trianion (Figure 12d) is similar to that of the tetraanion (Figure 12b) except that the trianion spectrum is shifted to higher binding energies with a threshold energy at 1.2 eV. Again at 266 nm, the higher binding energy features of the trianion spectrum disappear (Figure 12c). The photon-energy dependence of the PES features of both the tetra- and trianions is consistent with the existence of RCB's and the multiply charged nature of these species.

The observation of the negative binding energy in $[CuPc(SO_3)_4]^{4-}$ was not expected, because we know that the sulfonate groups are the charge carriers and they have very high electron

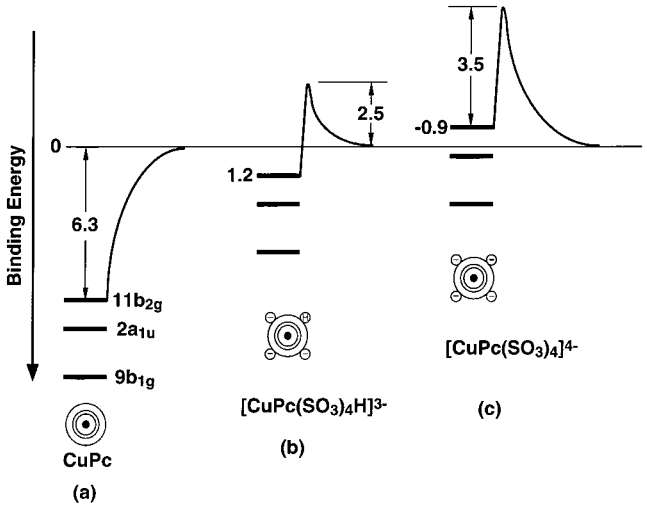

Figure 13. Schematic diagrams showing the top three molecular orbitals of the parent CuPc molecule and the rigid upshift of these orbitals due to the addition of three and four negative charges: (a) parent CuPc; (b) $[CuPc(SO_3)_4H]^{3-}$; (c) $[CuPc(SO_3)_4]^{4-}$. The cartons show the cyclic neutral CuPc molecule and the sequential charging at its periphery. Schematic potential energy curves for removing an electron from the highest occupied orbital of the respective species are shown, illustrating (a) the long-range attraction in the CuPc case, (b) the long-range Coulomb repulsion and the Coulomb barrier in the trianion, and (c) both the Coulomb barrier and the negative electron binding in the tetraanion. The experimentally determined electron binding energies and the Coulomb barrier heights in eV are indicated. The 6.3 eV ionization potential of CuPc is from ref 120. From ref 18.

binding energies. Our PES spectra of benzenesulfonate anion ($C_6H_5SO_3^-$) show two detachment features from the $-SO_3^-$ group separated by 0.6 eV with a threshold binding energy of ~5 eV.[20] In the tetraanion, the electron binding energy in $-SO_3^-$ is expected to be reduced due to the Coulomb repulsion from the other three negative charges. Figure 11 shows a schematic molecular structure of the tetraanion and the estimated distances between the charge centers and between the central Cu atom and the charge centers.[119] The $-SO_3^-$ group at position 1 experiences the largest Coulomb repulsion, which amounts to ~3.8 eV ($\sum_{n=2}^{4} e^2/R_{1n}$). Therefore, electrons on this $-SO_3^-$ group are still expected to be bound by at least 1.2 eV (5−3.8 eV). Thus we would not expect a negative binding energy if the HOMO of $[CuPc(SO_3)_4]^{4-}$ were derived from $-SO_3^-$.

However, we noted that the PES spectra of Figure 12b,d are rather similar to that of the neutral parent CuPc molecule in the vapor phase except that neutral CuPc has a much higher BE with a threshold ionization potential of 6.3 eV.[120] The similarity between the PES spectra of the charged species and that of the parent CuPc suggests that detachment occurs from molecular orbitals mainly of CuPc characters in the tetra- and trianions. This can be understood from the localized nature of the $-SO_3^-$ groups and the electrostatic interactions within the charged species. Previous density functional calculations predict that the HOMO of CuPc is a Cu d_π orbital with a single occupancy ($11b_{2g}$, Figure 13a).[121] An N p_π orbital ($2a_{1u}$, Figure 13a) is close to the HOMO. We estimated that the four negative charges would create a 7.2 eV ($\sum_{n=1}^{4} e^2/R_{n5}$) negative potential on the central Cu atom; i.e., an electron localized on Cu would experience a Coulomb repulsion of 7.2 eV. As schematically shown in Figure 13c, the HOMO of the CuPc will be shifted up by 7.2 eV, due to the Coulomb repulsion from the four negative charges on the peripheral $-SO_3^-$, giving rise to a −0.9 eV (6.3−7.2 eV) binding energy. This estimated binding energy is in perfect agreement with the experimental observation, despite the qualitative nature of the estimation. In the trianion, the most likely protonation position is to the $-SO_3^-$ group at position 1 (Figures 11 and 13b). The Coulomb repulsion to the central Cu due to the three charges at positions 2, 3, and 4 is now reduced to 5 eV ($\sum_{n=2}^{4} e^2/R_{n5}$), again in excellent agreement with the experimental observation that the trianion has a positive binding energy of 1.2 eV. Thus, we see a stepwise tuning of the HOMO of CuPc due to the charging at its periphery. Semiempirical calculations using the SPARTAN software package[20] show that indeed there is a stepwise rigid shift of the MO's of CuPc due to the negative charges and predict a negative binding energy for the HOMO of the tetraanion. The calculations further confirm that there is little mixing between the MO's of $-SO_3^-$ and CuPc and that the charges are indeed localized on the $-SO_3^-$ groups.

From the photon-energy-dependent spectral features, we estimated that the tri- and tetraanion possesses a RCB of 2.5 and 3.5 eV, respectively, as shown in Figure 13. The tetraanion can be viewed to store 0.9 eV excess electrostatic energy, which is unleashed during photodetachment and responsible for the seemingly puzzling fact that the photoelectron kinetic energy can be higher than the input photon energy. The tetraanion is thus electronically metastable and is expected to have a finite lifetime, which can be estimated with our ion-trap. We observed no measurable ion loss within a period of 400 s that we can store the ions. The long lifetime of this metastable tetraanion in the gas phase is also surprising and is attributed to the large barrier height and the large size of the molecule, such that the electron has to tunnel a long distance to escape. The RCB can be viewed as an electrostatic corral in this semiplanar molecule, trapping the negatively bound electron inside. These anions can thus be viewed as an electrostatic energy storage medium in the gas phase or a molecular capacitor. They can also be considered as a molecular analogue of a bulk charged metal surface, where the work function combined with the electric field around the metal surface creates a potential barrier (Schottky effect),[122] similar to that shown in Figure 13c. Finally, the current observation of tuning molecular energy levels by charging may also be relevant to the interactions of intense laser fields with atomic and molecular systems, leading to tunnel ionization.[123−125] In the latter, the strong electric field induced by a high power laser suppresses the Coulomb attraction for ionization and creates a potential barrier such that the electron can tunnel out (ionized). In the current tetraanion case, the four extra charges create a negative potential which is effectively higher than the ionization potential of the parent neutral CuPc. Despite the static nature of the electronic interactions in the multiply charged anion, the analogy between the two phenomena is interesting and may deserve further considerations.

3.5. Probing the Electronic Structure of Multiply Charged Transition Metal Complexes. There are many inorganic metal complexes that exist in solutions as MCA's.[126] These species have been studied extensively in the condensed phase. Gas phase studies of these metal complexes would be much desirable to obtain information about their intrinsic molecular properties without the complications of the condensed phase environments. The obtained molecular and spectroscopic information can be used to compare directly with theoretical calculations, which are often done on gaseous species. The apparatus that we developed is ideally suitable to study these species in the gas phase and obtain electronic structure information for any such metal complexes so long as they are long-lived in the gas phase.

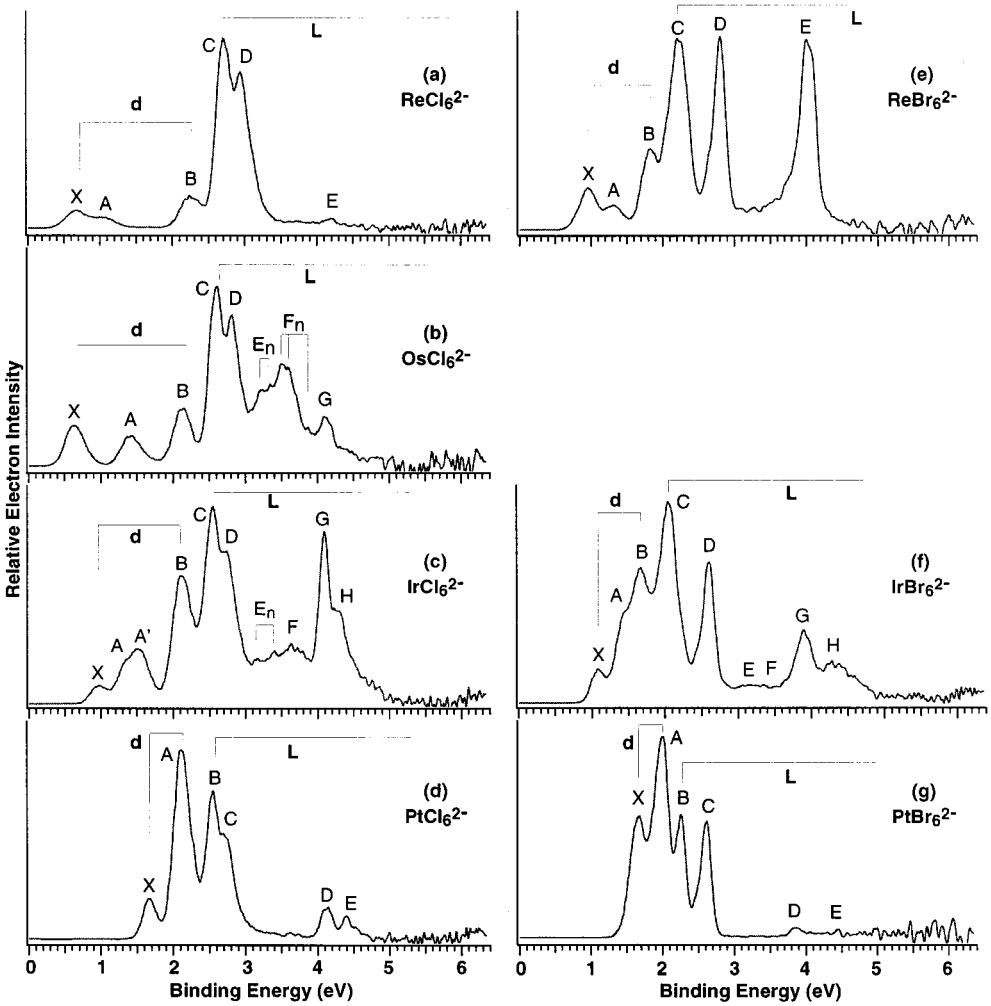

Figure 14. Photoelectron spectra of ML_6^{2-} (M = Re, Ir, Os, Pt; L = Cl, Br) at 193 nm. The labels "d" and "L" indicate features from metal d orbitals and ligand orbitals, respectively. From ref 17.

Our initial experimental effort to probe the electronic structure of inorganic metal complexes was focused on the octahedral or quasi-octahedral hexahalogenometalate species, MX_6^{2-} (M = Re, Os, Ir, Pt; X = Cl, Br).[17] These dianions are classical Werner-type transition metal complexes and are commonly found in the condensed phase.[126,127] These species are also interesting electron transfer agents in solutions and have been extensively studied as such.[128−139] There is also an extensive body of literature on the properties of these species in solids.[140−143] There have also been several theoretical investigations about the electronic and geometrical structures of these hexahalogenometalates.[144−146] However, there is no previous gas phase study on these species and it is not known if they are stable as free dianions or can be formed in the gas phase prior to our work.

We found that the hexahalogenometalate dianions can be made abundantly by electrospray of the corresponding potassium salt solutions, except for $OsBr_6^{2-}$, for which we found no commercial source for the needed salt compound. Figure 14 shows the PES spectra for the seven MX_6^{2-} dianions at 193 nm. All of these species were found to be stable as free gaseous doubly charged anions. We have also obtained the PES spectra of all the dianions at several lower detachment photon energies.[17] The photon-energy-dependent spectra clearly revealed the dianion nature of these species and allowed their RCB's to be estimated. The binding energies of the second excess electron in the dianions can be determined straightforwardly from the threshold detachment feature in each spectrum. A wealth of electronic structure information about these metal complexes was obtained, and low-lying and highly excited electronic states of the corresponding singly charged anions were observed, as shown in Figure 14. By comparing the spectral features of Cl complexes with those of the Br complexes, we can clearly distinguish detachment features from metal d orbitals or ligand orbitals, as labeled in Figure 14. We found that detachments from the metal d orbitals all occur at low binding energies whereas those from the ligand-dominated orbitals all take place at rather high binding energies.

For the four chloride anions, there has been a recent calculation by Macgregor and Moock.[139] Their calculated EA's for the monoanions, i.e., the binding energies of the second electron in the dianions, are consistent with our measured values and show the same trend (Figure 15), although the calculations in general underestimated the excess electron binding energies. In particular, the calculations gave a negative EA for $OsCl_6^-$; i.e., the calculation predicted that the $OsCl_6^{2-}$ dianion was not electronically stable, in contrast to our experimental observation.

We also found a remarkable correlation between electron affinities measured in vacuo and the redox potentials of these species in solution. An elementary oxidation reaction is a one-electron process and proceeds according to $[MX_6]^{2-} \rightarrow [MX_6]^- + e^-$, which, beside the solvation effects, is similar to electron detachment in the gas phase. Therefore, the gas phase EA's should be inherently related to the redox potentials, except that

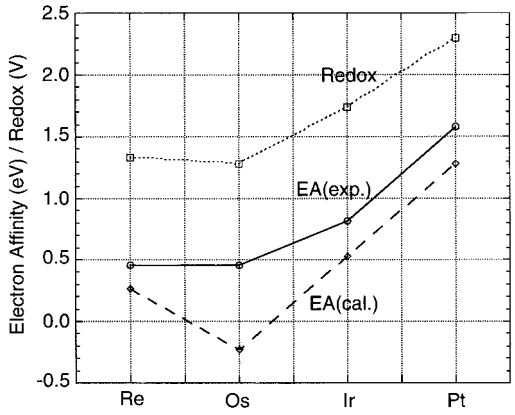

Figure 15. Correlation between measured (EA(exp.)) and calculated (EA(cal.))[139] adiabatic electron affinities of MCl_6^- (M = Re, Os, Ir, Pt) and the redox potentials of the corresponding dianions, MCl_6^{2-}, in solution.[139] From ref 17.

the solvation effects essential in redox processes in solution are missing in the electron detachment in a vacuum. In Figure 15, the redox potentials for MCl_6^{2-} (M = Re, OS, Ir, Pt) in solution[139] are compared with our measured EA's. It is seen clearly that there is a remarkable correlation between the gas-phase EA's for the hexachloride complexes and their redox potentials, suggesting that the solvation energies for all the relevant ions are probably similar in these cases. This is perhaps not surprising because the sizes of these anions, i.e., the M-Cl bond distances, are indeed very similar in the condensed phases.[139]

Many metal complexes can now be investigated in the gas phase using our experimental technique. Recently, we have obtained well-resolved PES spectra for the classical Werner complexes $PtCl_4^{2-}$ and $PtBr_4^{2-}$.[19] We have also obtained for the first time well-resolved spectra for the well-known metal complex containing a metal−metal multiple bond $[Re_2Cl_8]^{2-}$.[147] These data provide unprecedented experimental electronic structure information that would be valuable to verify the electronic structure models developed for these classical metal complexes.

3.6. Experimental Search for the Smallest Stable Gaseous Multiply Charged Anions. Different from ordinary molecules or singly charged anions, the stability of MCA's is entirely determined by the Coulomb repulsion between the excess charges. In order for a doubly charged anion to be stable, the Coulomb repulsion must be smaller than the electron affinity of the corresponding singly charged species (electronic stability) and the chemical bond strength against charge separation fragmentation (thermodynamic stability). To meet *both* conditions is difficult in small molecular species, requiring a delicate balance among the electron binding strength, chemical bond strength, and molecular structures. The smallest molecular entity that can bind two or more excess electrons with *both* electronic and thermodynamic stability is still an open question. There have been only a few convincing experimental observations of relatively small MCA's in the gas phase with less than 10 atoms, including C_n^{2-} ($n = 7-9$),[32−35] $S_2O_6^{2-}$,[43] $S_2O_8^{2-}$,[13,43] and very recently, SiC_n^{2-} ($n = 6, 8$),[42] BeF_4^{2-} and MgF_4^{2-},[41] and BeC_n^{2-} ($n = 4, 6, 8$).[40] The latter in fact was shown to be metastable.[40,41]

Among the MCA's with less than 7 atoms, there is now a consensus that no single atom can bind two or more excess electrons.[1,2] It has also been concluded that no diatomic or triatomic dianions are stable. The enormous Coulomb repulsion between the two excess charges in these small dianions makes them unstable against electron autodetachment. For tetraatomic systems, Sheller and Cederbaum predicted some of the smallest electronically stable MCA's consisting of alkali-metal halides (MX_3^{2-}).[63] However, these dianions were not observed in a recent experimental search, in which only pentaatomic BeF_4^{2-} and MgF_4^{2-} were turned up.[41] A recent theoretical calculation of LiF_3^{2-} indicates that it has very short lifetime at finite temperatures,[85] due to its thermodynamic instability against fragmentation ($LiF_3^{2-} \rightarrow LiF_2^- + F^-$). Boldyrev and Simons predicted that $Mg_2S_3^{2-}$ is likely to be the smallest electronically stable *linear* dianion.[78] Other pentaatomic MCA's that have been predicted to be electronically stable include alkaline-earth-metal halides (MX_4^{2-}),[64] among which BeF_4^{2-} and MgF_4^{2-} have been recently observed experimentally although they were shown to be metastable with finite lifetimes,[41] consistent with theoretical predictions that these species were thermodynamically unstable against fragmentation ($MX_4^{2-} \rightarrow MX_3^- + X^-$).[61,64,82,83] Among hexatomic systems, $M_2X_4^{2-}$-type of alkali-metal halides and $Si_2O_4^{2-}$ have been predicted to be electronically stable.[60,70] But again, the hexatomic $Li_2F_4^{2-}$ was not observed in the recent experimental search.[41]

We have engaged in an extensive experimental search for the smallest stable gaseous multiply charged anions.[19] Two types of small dianions were considered in this effort. The first includes the MX_4^{2-}-type of transition metal complexes (X = Cl, Br) that are known to exist in solutions.[126] The second type of dianions involved alkali-metal or alkaline-earth-metal halides species that are predicted theoretically to be electronically stable in the gas phase.[63−68] As pointed out in the Experimental Section, anions produced from our electrospray source were accumulated and stored in a quadrupole ion-trap for 0.1 s before being analyzed by the TOF mass spectrometer. Thus only MCA's with sufficiently long lifetimes (~0.1 s) can be observed in our experiments. For metastable MCA's, we can estimate their half-lives using the ion-trap. Since fluoride compounds have very low solubility in water or methanol, our search of the smaller alkali-metal and alkaline-earth-metal halide MCA's was focused mainly on the chloride and bromide complexes.

We did not observe the anticipated tetraatomic alkali--metal halide dianions, MX_3^{2-} (M = Li, Na, K; X = Cl, Br), the smallest dianions predicted to be electronically stable in the gas phase.[63] The hexatomic $M_2X_4^{2-}$-type of alkali-metal halide was also not observed. These findings are consistent with the recent search, which used a sputtering source.[41] We also failed to observe the pentaatomic alkaline-earth-metal halide dianions, MX_4^{2-} (M = Mg, Ca; X = Cl, Br), despite their longer predicted lifetimes. The recent observation of BeF_4^{2-} and MgF_4^{2-} put their lifetimes in the hundreds of microsecond range,[41] which would be too short for them to be observed in our experimental time scale.

For the transition metal tetrahalide complex dianions, MX_4^{2-} (X = Cl, Br), we searched all the 3d and group-10 elements. Much to our surprise, we could not observe any MX_4^{2-} species containing 3d elements, although many of these complexes exist in solutions.[126] Our only success came with the two heavier group-10 elements, Pd and Pt.[19] We observed abundant $PtCl_4^{2-}$ and $PtBr_4^{2-}$ dianions. The Pd-containing dianions were barely observable with very weak signals, in particular, for $PdCl_4^{2-}$. We could not search for the MX_4^{2-}-type of dianions for the other 4d- and 5d-elements because of the lack of appropriate precursor compounds.[126] They all prefer higher oxidation states (>+2), suggesting that the MX_4^{2-}-type of dianions probably do not exist for these other 4d- and 5d-elements.

Figure 16 shows the 266-nm PES spectra for the four observed dianions.[19] Surprisingly, $PtCl_4^{2-}$ and $PtBr_4^{2-}$ were

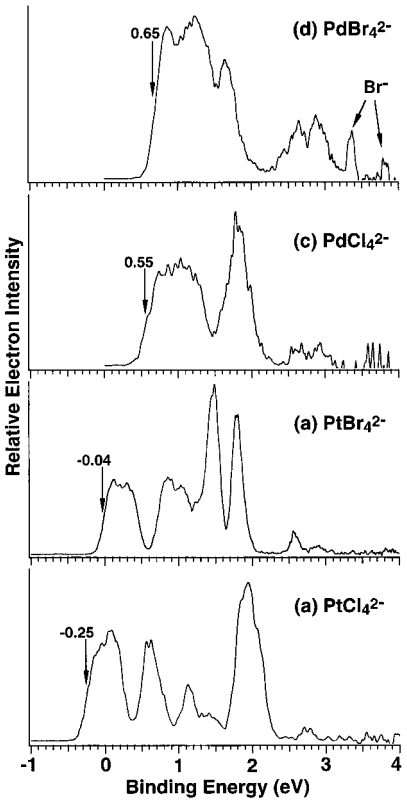

Figure 16. Photoelectron spectra of (a) $PtCl_4^{2-}$, (b) $PtBr_4^{2-}$, (c) $PdCl_4^{2-}$, and (d) $PdBr_4^{2-}$ at 266 nm (4.661 eV). The numbers and arrows indicate the estimated adiabatic electron binding energies with an uncertainty of ±0.05 eV. Note the negative binding energies revealed for $PtCl_4^{2-}$ and $PtBr_4^{2-}$. From ref 19.

found to have negative electron-binding energies, suggesting that they are electronically unstable (or metastable), whereas $PdCl_4^{2-}$ and $PdBr_4^{2-}$ gave positive electron-binding energies, suggesting that they are electronically stable species. To confirm the electronic metastability of $PtCl_4^{2-}$ and $PtBr_4^{2-}$, we further measured their lifetimes using the ion-trap. Within our experimental sensitivity, we estimated roughly a half-life of ~0.2 s for $PtCl_4^{2-}$. Similar measurements showed that $PtBr_4^{2-}$ has a much longer half-life of about ~60 s. We were also able to measure the lifetime of $PdBr_4^{2-}$ and were surprised to find that it was short-lived with a half-life of only ~8 s, suggesting that this dianion is actually *thermodynamically* unstable against fragmentation. The $PdCl_4^{2-}$ signal was too weak for us to perform any lifetime measurements. We thus attributed the very weak $PdCl_4^{2-}$ signal to its thermodynamic instability. From our experimental time scale, we inferred that its half-life should be less than 0.1 s.

The MX_3^{2-}-type of alkali-metal and MX_4^{2-}-type of alkaline-earth-metal halide dianions are predicted to be only stable electronically;[63,66] they are unstable thermodynamically against loss of a halide ion, due to the relatively weak metal−ligand bonding, which is essentially ionic in nature. Their lifetimes are determined by the magnitude of a potential barrier, analogous to the RCB for electron loss, along the fragmentation coordinate. The relatively weak bonding in the small alkali-metal and alkaline-earth-metal halide systems suggests that the potential barrier would be small in these dianions. A recent detailed lifetime calculation on LiF_3^{2-},[85] which has a relatively small barrier of ~0.2 eV, indicates that although it has a lifetime of $>10^{17}$ s at temperatures < 20 K, the lifetime falls below 10^{-5} s at 80 K. The electrospray source produces ions around or slightly above room temperature, which sets a practical limit for the observability of metastable dianions with relatively weak chemical bonding or small barriers. The current results suggest that even the enhanced metal−ligand bonding strength in the 3d MX_4^{2-} dianions relative to the alkaline-earth-metal species is not enough to render these dianions observable under our experimental conditions. It takes the enhanced bond strength of a 4d metal−ligand system to make the MX_4^{2-}-type of dianions to be sufficiently long-lived to be observed. It is also interesting to note that despite the superior electronic stability of the Pd complexes relative to the Pt complexes, it was much easier to observe the Pt complexes, due to their stronger metal−ligand bonding. Thus we see that the chemical bond strength is critical in determining the stability, lifetimes, and observablility of MCA's, because when considering MCA's one has to take into account *both* the electronic and thermodynamic stabilities. Although the four pentaatomic MCA's observed here,[19] as well as the other pentaatomic dianions observed recently,[41] are metastable after all, they set a practical lower size limit for the smallest *stable* (both electronically and thermodynamically) dianions in the gas phase.

4. The Future

We have shown in this overview some of the initial findings on gaseous multiply charged anions using photodetachment spectroscopy. These results demonstrate the power and versatility of the photodetachment technique to probe the properties of gaseous multiply charged anions. The investigation of free multiply charged anions is really still in its infantry, and it is fair to say that these initial efforts only represent the tip of an iceberg. First of all, the repulsive Coulomb barrier plays the most important role in determining the physical and chemical properties of multiply charged anions. The estimates using photon-energy-dependent PES in our studies are not precise. More accurate evaluations of the RCB's can be accomplished using tunable laser photodetachment, which will also allow more detailed characterization of the electron tunneling phenomenon as one tunes through the RCB and across the barrier top. Second, double electron detachment of a dianion with a single photon would be very interesting, although this channel will undoubtedly have low cross section. Such studies will provide unique opportunities to investigate electron correlation effects and dynamic electron−electron repulsion in MCA's. These experiments would require coincident detection of the two outgoing electrons or simply monitoring neutral products with a tunable laser. Third, photodetachment of multiply charged anions yields direct information about higher order electron affinities.[148] Very high first-order electron affinities have been predicted in a class of molecules called "superhalogens",[149−151] which possess electron affinities higher than the halogen atoms, the highest electron affinity atomic species. Very high electron binding energies have been predicted for a number of multiply charged "superhalogen" anions.[2,52−56,61−68,77,80−82] It would be interesting to confirm these predictions and search for "superhalogen anions",[19,148] i.e., anions with electron affinities higher than that of the halogens. Fourth, the photodetachment experiments presented here provide direct information about the electronic stability of MCA's, whereas thermodynamic stability can only be inferred indirectly by lifetime measurements. Photofragmentation or collision-induced dissociation of MCA's (Coulomb explosion) will yield direct thermodynamic information about the MCA's, such as the barrier to bond dissociation, bond strength, and energetic information.

More exciting is the prospect that we now have available to us a means to investigate solution phase chemistry and species

in the gas phase. For example, we have observed abundant ion-pair and salt-bridge complexes,[14,152] which are important in understanding properties of electrolyte solutions. Solvation effects and solvent stabilization of MCA's are other issues important to solution phase chemistry and can be addressed with the techniques described here.[12] How many solvent molecules are needed to stabilize an otherwise unstable MCA in the gas phase? Answers to this question not only provide information about the stability and energetics about the MCA but also molecular information about the microsolvation of the MCA in solution. Other significant issues of solution chemistry that may be addressed by photodetachment include energetics of H-bonded species, in particular, species with intramolecular H-bonding, and energetics and electronic structure information about electron-transfer reactions, organic anions and free radicals, and even DNA's and proteins. Just as the supersonic beam technique has revolutionized the study of chemical reaction dynamics under well-controlled reaction conditions, the electrospray technique provides yet another tool that has the promise to open up a whole new realm of investigation of solution phase phenomena in the gas phase with molecular details and specificity.

Acknowledgment. The work described in this article has been supported by several sources. These include the National Science Foundation under Grant CHE-9817811, the Petroleum Research Fund, administered by the American Chemical Society, and the U.S. Department of Energy, Office of Basic Energy Sciences, Chemical Science Division. The work was performed at the W. R. Wiley Environmental Molecular Sciences Laboratory, a national scientific user facility sponsored by DOE's Office of Biological and Environmental Research and located at Pacific Northwest National Laboratory, which is operated for DOE by Battelle under Contract No. DE-AC06-76RLO 1830. L.S.W. is an Alfred P. Sloan Research Fellow.

References and Notes

(1) Compton, R. N. Negative Ion States. In *Photophysics and Photochemistry in the Vacuum Ultraviolet*; McGlynn, S. P., et al., Eds.; Reidel: Dordrecht, The Netherlands, 1985.
(2) Scheller, M. K.; Compton, R. N.; Cederbaum, L. S. *Science* **1995,** *270*, 1160.
(3) Jin, C.; Hettich, R. L.; Compton, R. N.; Tuinman, A. A.; Derecskei-Kovacs, A.; Marynick, D. S.; Dunlap, B. I. *Phys. Rev. Lett.* **1994**, *73*, 2821.
(4) Compton, R. N.; Tuinman, A. A.; Klots, C. E.; Pederson, M. R.; Patton, D. C. *Phys. Rev. Lett.* **1997**, *78*, 4367.
(5) Yannouleas, C.; Landman, U. *Chem. Phys. Lett.* **1993**, *210*, 437.
(6) Yannouleas, C.; Landman, U. *Chem. Phys. Lett.* **1994**, *217*, 175.
(7) Martin, R. L.; Ritchie, J. P. *Phys. Rev. B* **1993**, *48*, 4845.
(8) See for example: Hodgson, P. E.; Gadioli, E.; Erba, E. G. *Introductory Nuclear Physics*; Clarendon Press: Oxford, U.K., 1997.
(9) Wigner, E. P. *Phys. Rev.* **1948**, *73*, 1003.
(10) Wang, X. B.; Ding, C. F.; Wang, L. S. *Phys. Rev. Lett.* **1998**, *81*, 3351.
(11) Wang, L. S.; Ding, C. F.; Wang, X. B.; Nicholas, J. B. *Phys. Rev. Lett.* **1998**, *81*, 2667.
(12) Ding, C. F.; Wang, X. B.; Wang, L. S. *J. Phys. Chem. A* **1998**, *102*, 8633.
(13) Ding, C. F.; Wang, X. B.; Wang, L. S. *J. Chem. Phys.* **1999**, *110*, 3635.
(14) Wang, X. B.; Ding, C. F.; Nicholas, J. B.; Dixon, D. A.; Wang, L. S. *J. Phys. Chem. A* **1999**, *103*, 3423.
(15) Wang, X. B.; Ding, C. F.; Wang, L. S. *Chem. Phys. Lett.* **1999**, *307*, 391.
(16) Wang, L. S.; Ding, C. F.; Wang, X. B.; Barlow, S. E. *Rev. Sci. Instrum.* **1999**, *70*, 1957.
(17) Wang, X. B.; Wang, L. S. *J. Chem. Phys.* **1999**, *111*, 4497.
(18) Wang, X. B.; Wang, L. S. *Nature* **1999**, *400*, 245.
(19) Wang, X. B.; Wang, L. S. *Phys. Rev. Lett.* **1999**, *83*, 3402; *J. Am. Chem. Soc.*, in press.
(20) Wang, X. B.; Ferris, K.; Wang, L. S. *J. Phys. Chem. A* **2000**, *104*, 25.
(21) Wang, L. S. *Comments At. Mol. Phys.* **2000**, in press.
(22) Kalcher, J.; Sax, A. F. *Chem. Rev.* **1994**, *94*, 2291.
(23) Freeman, G. R.; March, N. H. *J. Phys. Chem.* **1996**, *100*, 4331.
(24) Compton, R. N. Multiply Charged Negative Ions. In *Negative Ions*; Esaulov, V., Ed.; Cambridge University Press: Cambridge, U.K., 1996.
(25) Schroder, D.; Schwarz, H. *J. Phys. Chem. A* **1999**, *103*, 7385.
(26) Dougherty, R. C. *J. Chem. Phys.* **1969**, *50*, 1896.
(27) Bowie, J. H.; Stapleton, B. J. *J. Am. Chem. Soc.* **1976**, *98*, 6480.
(28) Bruins, A. P.; Covey, T. R.; Henion, J. D. *Anal. Chem.* **1987**, *59*, 2642.
(29) Weidolf, L. G.; Lee, E. D.; Henion, J. D. *Biomed. Environ. Mass Spectrom.* **1988**, *15*, 283.
(30) Maas, W. P. M.; Nibbering, N. M. M. *Int. J. Mass Spectrom. Ion Processes* **1989**, *88*, 257.
(31) Leiter, K.; Ritter, W.; Stamatovic, A.; Mark, T. D. *Int. J. Mass Spectrom. Ion Processes* **1986**, *68*, 341.
(32) Schauer, S. N.; Williams, P.; Compton, R. N. *Phys. Rev. Lett.* **1990**, *65*, 625.
(33) Gnaser, H.; Oechsner, H. *Nucl. Instr. Methods Phys. Res. B* **1993**, *82*, 518.
(34) Middleton, R.; Klein, J. *Nucl. Instrum. Methods Phys. Res. B* **1997**, *123*, 532.
(35) Calabrese, D.; Covington, A. M.; Thompson, J. S. *J. Chem. Phys.* **1996**, *105*, 2936.
(36) Mathur, D.; Bhardwaj, V. R.; Rajgara, F. A.; Safvan, C. P. *Chem. Phys. Lett.* **1997**, *277*, 558.
(37) Hettich, R. L.; Compton, R. N.; Rotchie, R. H. *Phys. Rev. Lett.* **1991**, *67*, 1242.
(38) Limbach, P. A.; Schweikhard, L.; Cowen, K. A.; McDermott, M. T.; Marshall, A. G.; Coe, J. V. *J. Am. Chem. Soc.* **1991**, *113*, 6795.
(39) Boltalina, O. V.; Hvelplund, P.; Larsen, M. C.; Larsson, M. O. *Phys. Rev. Lett.* **1998**, *80*, 5102.
(40) Middleton, R.; Klein, J. *Nucl. Instrum. Methods Phys. Res. B* **1999**, *159*, 8.
(41) Middleton, R.; Klein, J. *Phys. Rev. A* **1999**, *60*, 3515.
(42) Gnaser, H. *Phys. Rev. A* **1999**, *60*, R2645.
(43) Blades, A. T.; Kebarle, P. *J. Am. Chem. Soc.* **1994**, *116*, 10761.
(44) Blades, A. T.; Klassen, J. S.; Kebarle, P. *J. Am. Chem. Soc.* **1995**, *117*, 10563.
(45) Blades, A. T.; Ho, Y.; Kebarle, P. *J. Phys. Chem.* **1996**, *100*, 2443.
(46) Lau, T. C.; Wang, J.; Siu, K. W. M.; Guevremont, R. *J. Chem. Soc., Chem. Commun.* **1994**, 1487.
(47) Lau, T. C.; Wang, J.; Guevremont, R.; Siu, K. W. M. *J. Chem. Soc., Chem. Commun.* **1995**, 877.
(48) Khairallah, G.; Peel, J. B. *J. Phys. Chem. A* **1997**, *101*, 6770.
(49) Khairallah, G.; Peel, J. B. *Chem. Phys. Lett.* **1997**, *268*, 218.
(50) Khairallah, G.; Peel, J. B. *Chem. Phys. Lett.* **1998**, *296*, 545.
(51) Tuinman, A. A.; Compton, R. N. *J. Phys. Chem. A* **1998**, *102*, 9791.
(52) Miyoshi, E.; Sakai, Y. *J. Chem. Phys.* **1988**, *89*, 7363.
(53) Miyoshi, E.; Sakai, Y.; Murakami, A.; Iwaki, H.; Tereshima, H.; Shoda, T.; Kawaguchi, T. *J. Chem. Phys.* **1988**, *89*, 4193.
(54) Gutsev, G. L.; Boldyrev, A. I. *J. Phys. Chem.* **1990**, *94*, 2256.
(55) Gutsev, G. L. *Chem. Phys. Lett.* **1991**, *184*, 305.
(56) Ewig, C. S.; Van Wazer, J. R. *J. Am. Chem. Soc.* **1990**, *112*, 109.
(57) Korobov, M. V.; Kuznetsov, S. V.; Sidorov, L. N.; Shipachev, V. A.; Mit'kin, V. N. *Int. J. Mass Spectrom. Ion Phys.* **1989**, *87*, 13.
(58) Hotokka, M.; Pyykko, P. *Chem. Phys. Lett.* **1989**, *157*, 415.
(59) Pyykko, P.; Zhao, Y. F. *J. Phys. Chem.* **1990**, *94*, 7753.
(60) Pyykko, P.; Runeberg, N. *Chem. Commun.* **1991**, 547.
(61) Weikert, H. G.; Cederbaum, L. S.; Tarantelli, F.; Boldyrev, A. I. *Z. Phys. D* **1991**, *18*, 299.
(62) Sommerfeld, T.; Scheller, M. K.; Cederbaum, L. S. *Chem. Phys. Lett.* **1993**, *209*, 216.
(63) Scheller, M. K.; Cederbaum, L. S. *J. Chem. Phys.* **1993**, *99*, 441.
(64) Weikert, H. G.; Cederbaum, L. S. *J. Chem. Phys.* **1993**, *99*, 8877.
(65) Scheller, M. K.; Cederbaum, L. S. *Chem. Phys. Lett.* **1993**, *216*, 141.
(66) Scheller, M. K.; Cederbaum, L. S. *J. Chem. Phys.* **1994**, *100*, 8934.
(67) Scheller, M. K.; Cederbaum, L. S. *J. Chem. Phys.* **1994**, *100*, 8943.
(68) Scheller, M. K.; Cederbaum, L. S. *J. Chem. Phys.* **1994**, *101*, 3962.
(69) Sommerfeld, T.; Scheller, M. K.; Cederbaum, L. S. *J. Phys. Chem.* **1994**, *98*, 8914.
(70) Sommerfeld, T.; Scheller, M. K.; Cederbaum, L. S. *J. Chem. Phys.* **1995**, *103*, 1057.
(71) Sommerfeld, T.; Scheller, M. K.; Cederbaum, L. S. *J. Chem. Phys.* **1996**, *104*, 1464.
(72) Weikert, H. G.; Meyer, H. D.; Cederbaum, L. S. *J. Chem. Phys.* **1996**, *104*, 7122.
(73) Sommerfeld, T.; Riss, U. V.; Meyer, H. D.; Cederbaum, L. S. *Phys. Rev. Lett.* **1997**, *79*, 1237.
(74) Berghof, V.; Sommerfeld, T.; Cederbaum, L. S. *J. Phys. Chem. A* **1998**, *102*, 5100.
(75) Dreuw, A.; Sommerfeld, T.; Cederbaum, L. S. *J. Chem. Phys.* **1998**, *109*, 2727.

(76) Dreuw, A.; Cederbaum, L. S. *J. Chem. Phys*. **1999**, *111*, 1467.
(77) Boldyrev, A. I.; Simons, J. *J. Chem. Phys*. **1992**, *97*, 2826.
(78) Boldyrev, A. I.; Simons, J. *J. Chem. Phys*. **1993**, *98*, 4745.
(79) Boldyrev, A. I.; Simons, J. *J. Phys. Chem*. **1994**, *98*, 2293.
(80) Gutowski, M.; Boldyrev, A. I.; Ortiz, J. V.; Simons, J. *J. Am. Chem. Soc*. **1994**, *116*, 9262.
(81) Gutowski, M.; Boldyrev, A. I.; Simons, J.; Rak, J.; Blazejowski, J. *J. Am. Chem. Soc*. **1996**, *118*, 1173.
(82) Boldyrev, A. I.; Gutowski, M.; Simons, J. *Acc. Chem. Res*. **1996**, *29*, 497.
(83) Stefanovich, E. V.; Boldyrev, A. I.; Truong, T. N.; Simons, J. *J. Phys. Chem. B* **1998**, *102*, 4205.
(84) McKee, M. L. *J. Phys. Chem*. **1996**, *100*, 3473.
(85) Sommerfeld, T.; Child, M. S. *J. Chem. Phys*. **1999**, *110*, 5670.
(86) Adamowicz, L. *J. Chem. Phys*. **1991**, *95*, 8669.
(87) Watts, J. D.; Bartlett, R. J. *J. Chem. Phys*. **1992**, *97*, 3445.
(88) Zakrzewski, V. G.; Ortiz, J. V. *J. Chem. Phys*. **1995**, *102*, 294.
(89) Enlow, M.; Ortiz, J. V.; Luthi, H. P. *Mol. Phys*. **1997**, *92*, 441.
(90) Dolgounitcheva, O.; Zakrzewski, V. G.; Ortiz, J. V. *J. Chem. Phys*. **1998**, *109*, 87.
(91) Gutowski, M.; Rak, J.; Dokurno, P.; Blazejowski, J. *Inorg. Chem*. **1994**, *33*, 6187.
(92) Gutowski, M.; Rak, J.; Dokurno, P.; Blazejowski, J. *J. Phys. Chem*. **1994**, *98*, 6280.
(93) Rak, J.; Gutowski, M.; Dokurno, P.; Thanh, H. V.; Blazejowski, J. *J. Chem. Phys*. **1994**, *100*, 5810.
(94) Drake, G. W.; Dixon, D. A.; Sheehy, J. A.; Boatz, J. A.; Christe, K. O. *J. Am. Chem. Soc*. **1998**, *120*, 8392.
(95) Arratia-Perez, R.; Hernandez-Acevedo, L. *J. Chem. Phys*. **1999**, *111*, 168.
(96) Akdeniz, Z.; Cicek, Z.; Tosi, M. P. *Chem. Phys. Lett*. **1999**, *308*, 479.
(97) Rubio, A.; Balbas, L. C.; Alonso, J. A. *Physica B* **1990**, *167*, 19.
(98) Peterson, M. R.; Quong, A. A. *Phys. Rev. B* **1992**, *46*, 13584.
(99) Chang, A. H. H.; Ermler, W. C.; Pitzer, R. M. *J. Phys. Chem*. **1991**, *95*, 9288.
(100) Turner, D. W.; Baker, C.; Baker, A. D.; Bundle, C. R. *Molecular Photoelectron Spectroscopy*; Wiley: New York, 1970.
(101) Rabalais, J. W. *Principles of Ultraviolet Photoelectron Spectroscopy*; Wiley: New York, 1977.
(102) Eland, J. H. D. *Photoelectron Spectroscopy*, 2nd ed.; Butterworth: London, 1984.
(103) Hotop, H.; Lineberger, W. C. *J. Phys. Chem. Ref. Data* **1985**, *14*, 731.
(104) Leopold, D. G.; Lineberger, W. C. *J. Chem. Phys*. **1986**, *81*, 51.
(105) McHugh, K. M.; Eaton, J. G.; Lee, G. H.; Sarkas, H. W.; Kidder, L. H.; Snodgrass, J. T.; Manaa, M. R.; Bowen, K. H. *J. Chem. Phys*. **1989**, *91*, 3792.
(106) Cheshnovsky, O.; Yang, S. H.; Pettiette, C. L.; Craycraft, M. J.; Smalley, R. E. *Rev. Sci. Instrum*. **1987**, *58*, 2131.
(107) Gantefor, G.; Meiwes-Broer, K. H.; Lutz, H. O. *Phys. Rev. A* **1988**, *37*, 2716.
(108) Casey S. M.; Leopold, D. G. *J. Phys. Chem*. **1993**, *97*, 816.
(109) Kitsopoulos, T. N.; Chick, C. J.; Zhao, Y.; Neumark, D. M. *J. Chem. Phys*. **1991**, *95*, 1441.
(110) Wang, L. S.; Cheng, H. S.; Fan, J. *J. Chem. Phys*. **1995**, *102*, 9480.
(111) Yamashita, M.; Fenn, J. B. *J. Phys. Chem*. **1984**, *88*, 4451.
(112) Yamashita, M.; Fenn, J. B. *J. Phys. Chem*. **1984**, *88*, 4671.
(113) Fenn, J. B.; Mann, M.; Meng, C. K.; Wong, S. F.; Whitehouse, C. M. *Science* **1989**, *246*, 64.
(114) Snyder, A. P., Ed. *Biochemical and Biotechnological Applications of Electrospray Ionization Mass Spectrometry*; American Chemical Society: Washington, DC, 1995.
(115) Weast, R. C., et al., Eds. *CRC Handbook of Chemistry and Physics*, 67th ed.; CRC Press: Boca Raton, FL, 1986.
(116) Gross, D. S.; Rodriguez-Cruz, S. E.; Bock, S.; Williams, E. R. *J. Phys. Chem*. **1995**, *99*. 4034.
(117) Gronert, S. *Int. J. Mass Spectrom*. **1999**, *185*, 351.
(118) Comptom, R. N. Private communication.
(119) Brown, C. J. *J. Chem. Soc. A* **1968**, 2488.
(120) Berkowitz, J. *J. Chem. Phys*. **1979**, *70*, 2819.
(121) Rosa, A.; Baerends, E. J. *Inorg. Chem*. **1994**, *33*, 584.
(122) D'Haennens, I. J. In *Encyclopedia of Physics*; Lerner, R. G., Trigg, G. L., Eds.; VCH: New York, 1991; p 1251.
(123) Ilkov, F. A.; Decker, J. E.; Chin, S. L. *J. Phys. B* **1992**, *25*, 4005.
(124) Walsh, T. D. G.; Ilkov, F. A.; Decker, J. E.; Chin, S. L. *J. Phys. B* **1994**, *27*, 3767.
(125) Levis, R. J.; DeWitt, M. J. *J. Phys. Chem. A* **1999**, *103*, 6493.
(126) Cotton, F. A.; Wilkinson, G. *Advanced Inorganic Chemistry*; Wiley: New York, 1988.
(127) Bray, M. R.; Deeth, R. J.; Paget, V. J.; Sheen, P. D. *Int. J. Quantum Chem*. **1996**, *61*, 85.
(128) Gardner, H. C.; Kochi, J. K. *J. Am. Chem. Soc*. **1975**, *97*, 1855.
(129) Chen, J. Y.; Kochi, J. K. *J. Am. Chem. Soc*. **1977**, *99*, 1450.
(130) Wong, C. L.; Kochi, J. K. *J. Am. Chem. Soc*. **1979**, *101*, 5593.
(131) Doona, C. J.; Stanbury, D. M. *Inorg. Chem*. **1996**, *35*, 3210.
(132) Ghosh, M. C.; Mandal, S.; Chandra, S. K.; Gould, E. S. *Inorg. Chem*. **1995**, *34*, 509.
(133) Hung, M.-L.; McKee, M. L.; Stanbury, D. M. *Inorg. Chem*. **1994**, *33*, 5108.
(134) Jimenez, R.; Graciani, M. M.; Rodriguez, A.; Moya, M. L.; Sanchez, M. F.; Lopez-Cornejo, P. *Langmuir* **1997**, *13*, 187.
(135) Lay, P. A.; Taube, H. *Inorg. Chem*. **1989**, *28*, 3561.
(136) Dehnicke, K.; Muller, U.; Weber, R. *Inorg. Chem*. **1984**, *23*, 2563.
(137) Li, Q.; Chen, Z.; Zheng, X.; Jin, Z. *J. Phys. Chem*. **1992**, *96*, 5959.
(138) Shulpin, G. B.; Nizova, G. V.; Shilov, A. E. *J. Chem. Soc., Chem. Commun*. **1983**, 672.
(139) Macgregor, S. A.; Moock, K. H. *Inorg. Chem*. **1998**, *37*, 3284.
(140) Sleight, T. P.; Hare, C. R. *J. Phys. Chem*. **1968**, *72*, 2207.
(141) McCaffery, A. J.; Rowe, M. D.; Rice, D. A. *J. Chem. Soc., Dalton Trans*. **1973**, 1605.
(142) Cox, L. E.; Hercules, D. M. *J. Electron Spectrosc. Relat. Phenom*. **1973**, *1*, 193.
(143) Kim, E. E.; Eriks, K.; Magnuson, R. *Inorg. Chem*. **1984**, *23*, 393.
(144) Cotton, F. A.; Harris, C. B. *Inorg. Chem*. **1967**, *6*, 376.
(145) Goursot, A.; Chermette, H.; Daul, C. *Inorg. Chem*. **1984**, *23*, 305.
(146) Deeth, R. J.; Jenkins, H. D. B. *J. Phys. Chem. A* **1997**, *101*, 4793.
(147) Wang, X. B.; Wang, L. S. *J. Am. Chem. Soc*., in press.
(148) Wang, X. B.; Wang, L. S. *J. Phys. Chem. A*, submitted for publication.
(149) Gutsev, G. L.; Boldyrev, A. I. *Chem. Phys*. **1981**, *56*, 277.
(150) Gutsev, G. L.; Boldyrev, A. I. *Chem. Phys. Lett*. **1984**, *108*, 250.
(151) Gutsev, G. L.; Boldyrev, A. I. *Adv. Chem. Phys*. **1985**, *61*, 169.
(152) Wang, X. B.; Ding, C. F.; Wang, L. S.; Boldyrev, A. I.; Simons, J. *J. Chem. Phys*. **1999**, *110*, 4763.